SUPPLEMENTAL DATA

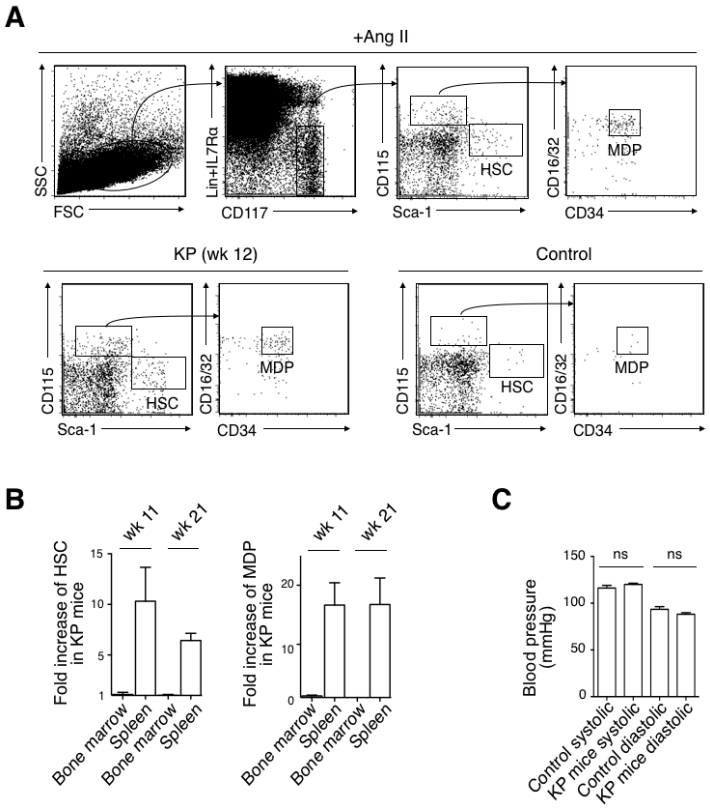

Figure S1 – HSC and MDP responses induced by AngII and lung adenocarcinomas (related to Figure 1).

(A) Gating scheme for identification of splenic HSCs and MDPs by flow cytometry. Top: mice infused with AngII (+AngII); bottom left: tumor bearing KP mice at 12 weeks post tumor initiation (KP); bottom right: untreated mice (Control).

(B) Fold change in the number of HSCs (left) and MDPs (right) in the bone marrow and spleen of tumor-bearing KP mice at week 11 (wk 11, n=14) and at week 21 (wk 21, n= 4) post tumor initiation, and compared to age-matched tumor free mice (average from n=9).

(C) Systolic and diastolic blood pressures in control mice (Control, n=5 animals with 3 independent measurements per animal) and tumor-bearing KP mice at 11 wk post tumor initiation (KP, n=5 animals with 4 independent measurements per animal).

Data are presented as mean ± SEM. ns = not significant.

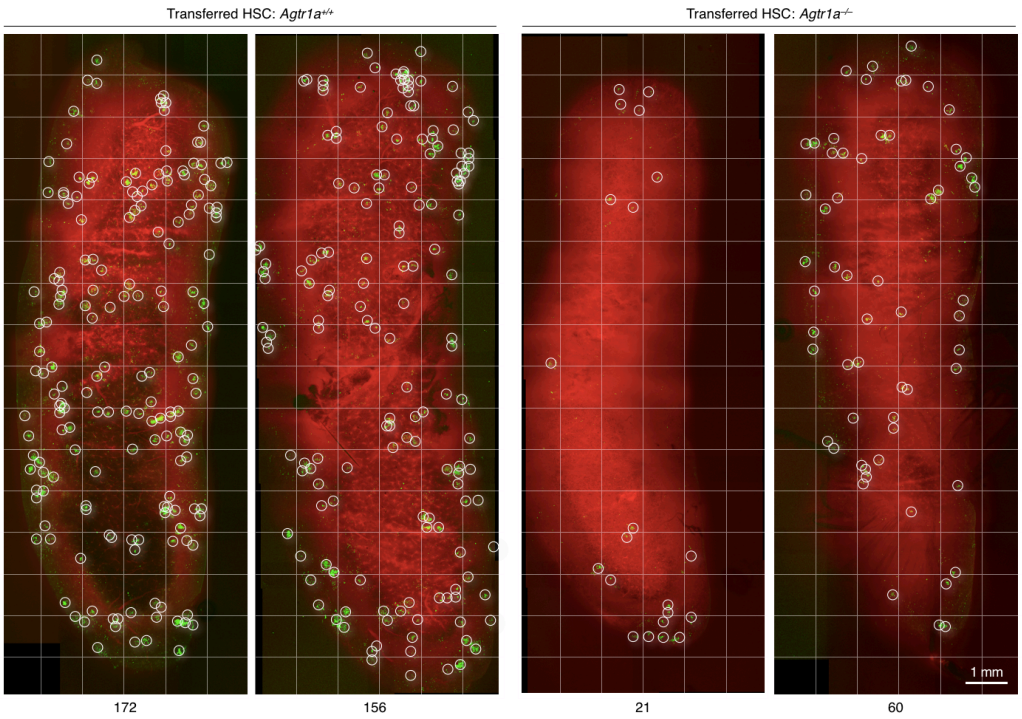

Figure S2 – *In vivo* fate mapping of *Agtr1a*$^{+/+}$ and *Agtr1a*$^{-/-}$ HSC progeny (related to Figure 2).

Intravital confocal micrographs of the splenic red pulp from wild-type mice infused with AngII for 7 d. EGFP^{+} *Agtr1a*$^{+/+}$ (left, 2 mice) or EGFP^{+} *Agtr1a*$^{-/-}$ (right, 2 mice) HSCs were injected i.v. 2 d after implantation of the AngII minipumps and imaging was done 5 d post adoptive transfer. EGFP^{+} cell clusters (green) are highlighted in circles. Total number of clusters are shown below each image. Scale bar represents 1 mm.

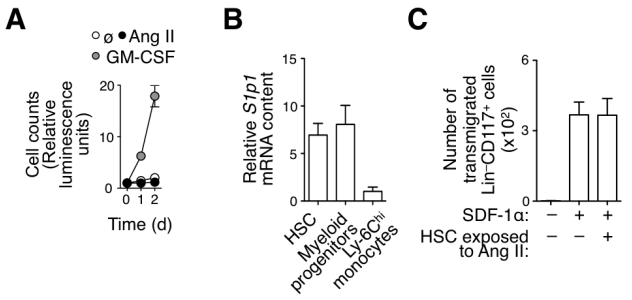

Figure S3 – HSC proliferation, *S1p1* expression and chemotaxis toward SDF-1α (related to Figure 3).

(A) *In vitro* proliferation assay of purified HSCs cultured in the presence of AngII (10 μM), GM-CSF (1 ng/ml) or in control medium (ø). The assay was done in triplicate and data are representative of 2 independent experiments.

(B) Relative *S1p1* mRNA content in FACS-purified splenic HSCs (n=6), myeloid progenitors (n=6) and Ly-6C^{hi} monocytes (n=9) obtained from wild-type mice.

(C) *Ex vivo* chemotaxis of splenic Lin$^-$ CD117$^+$ cells toward SDF-1α gradients. The Lin$^-$CD117$^+$ cells were obtained from mice that were previously exposed, or not, to AngII *in vivo* (n=4 for all groups). The cells were purified by FACS and analyzed *ex vivo* in a chemotaxis assay.

Data are presented as mean ± SEM.

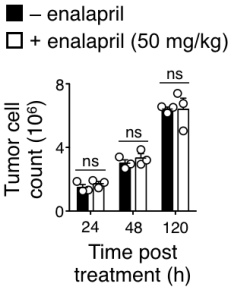

Figure S4 – Enalapril does not impair KP tumor cell growth *in vitro* (related to Figure 4).

KP tumor cells (4 x 10^5) were cultured either in control medium (– enalapril; black bars; n=3) or in medium supplemented with 50 mg/kg enalapril (+ enalapril; white bars; n=3). Cells were counted at 24, 48, and 120 h post initiation of enalapril treatment.

Data are presented as mean ± SEM. ns= not significant.

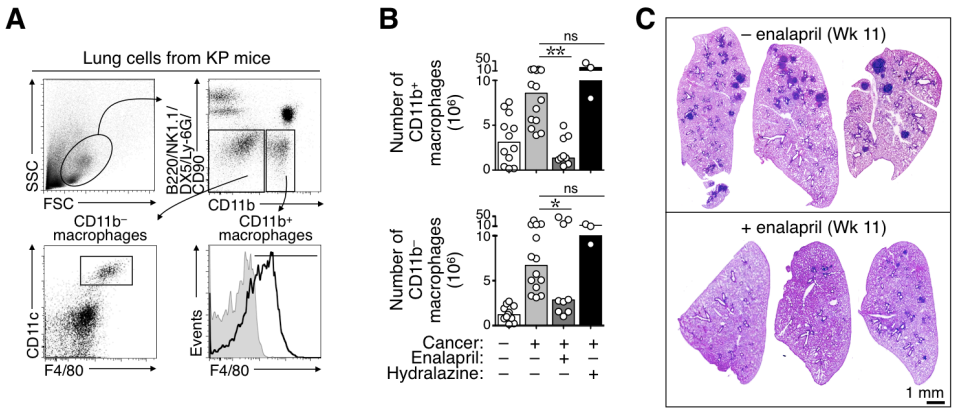

Figure S5 – Blockade of AngII production suppresses the TAM response (related to Figure 5).

(A) Gating scheme for identification of CD11b$^+$ and CD11b$^-$ macrophages in mouse lungs by flow cytometry.

(B) Quantification of CD11b$^+$ (top) and CD11b$^-$ (bottom) lung macrophages in four cohorts or mice: From left to right: age-matched tumor-free control mice (–Cancer, n=13); tumor-bearing KP mice (+Cancer, n=13); KP mice treated with enalapril (+Cancer +Enalapril; n=8); KP mice treated with hydralazine (+Cancer +Hydralazine; n=3). Tumor-bearing mice were analyzed at 11 wk post tumor initiation. Treatment with enalapril or hydralazine started at wk 8. Bar histograms show median values and dots represent single mice.

(C) Hematoxylin and eosin staining of lung tissue from KP mice at 11 wk post tumor initiation. Mice were either untreated (top; – enalapril; n=3) or started enalapril treatment at wk 8 (bottom; + enalapril; n=3). Data are representative of two independent experiments. Scale bar represents 1 mm.

Data are presented as mean ± SEM. *, p<0.05; **, p<0.01; ns= not significant.

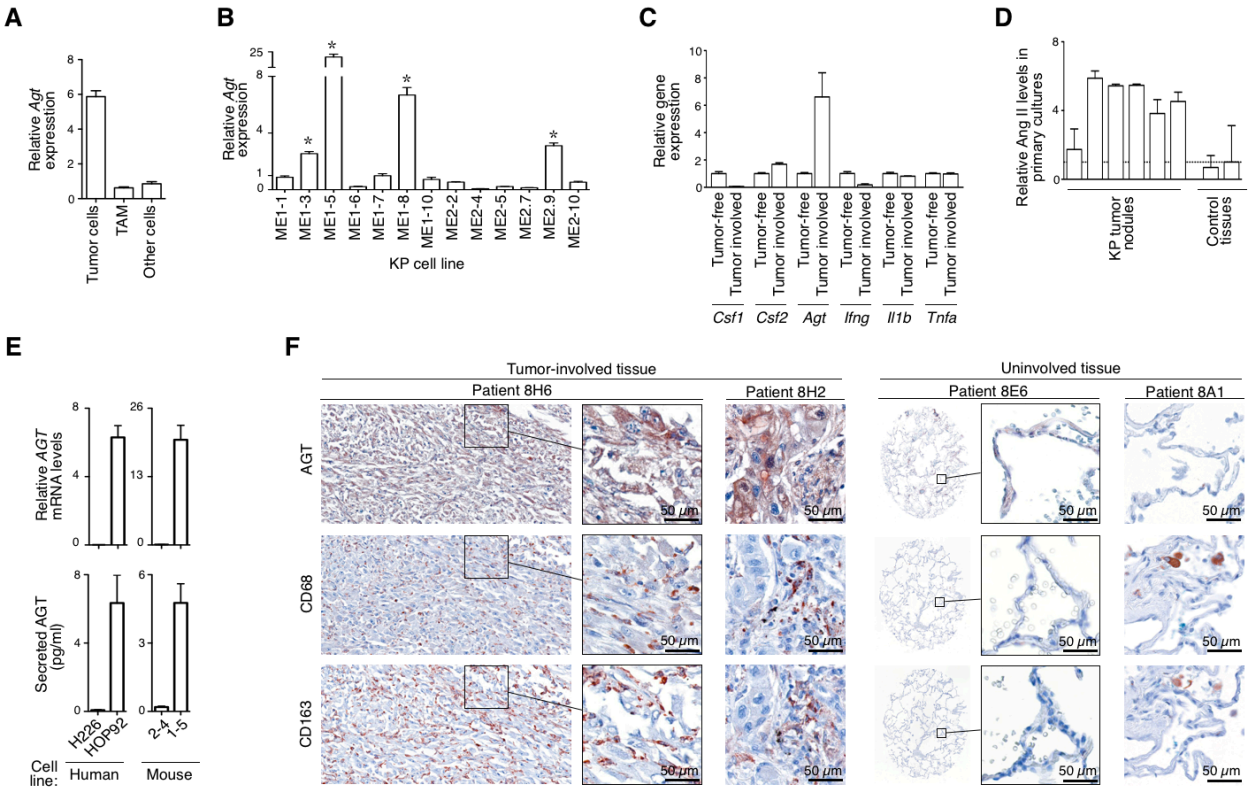

Index	NSCLC subtype	Fold change	p-value	Gene rank	Reference
1	Lung Adenocarcinoma	1.538	0.029	1319 (top 25%)	Beer, 2002
2	Lung Adenocarcinoma	-1.553	0.870	4316 (top 51%)	Bhatta-charjee, 2001
3	Large Cell Lung Carcinoma	1.567	0.103	3485 (top 32%)	Garber, 2001
4	Lung Adenocarcinoma	3.121	0.003	1156 (top 11%)	Garber, 2001
5	Large Cell Lung Carcinoma	3.903	0.001	4108 (top 21%)	Hou, 2010
6	Lung Adenocarcinoma	1.890	0.000355	4602 (top 24%)	Hou, 2010
7	Lung Adenocarcinoma	1.412	0.0000274	2406 (top 20%)	Landi, 2008
8	Lung Adenocarcinoma	1.866	0.052	2636 (top 31%)	Stearman, 2005
9	Lung Adenocarcinoma	1.735	0.0000351	616 (top 5%)	Su, 2007
10	Large Cell Lung Carcinoma	-1.151	0.968	2195 (top 88%)	Yamagata, 2003
11	Lung Adenocarcinoma	-1.172	0.927	2072 (top 83%)	Yamagata, 2003

Figure S6 – AGT over-expression in mouse and a subset of human NSCLC (related to Figure 6).

(A) Relative *Agt* mRNA expression levels (quantitative real time PCR) in FACS-sorted tumor cells, TAMs and other cells obtained from lung tissue of tumor-bearing mice. Data are normalized to *Agt* mRNA expression levels in control lung tissue.

(B) Relative *Agt* mRNA expression levels (quantitative real time PCR) in 13 tumor cell lines derived from lungs of KP mice. Data are normalized to *Agt* mRNA expression levels in control lung tissue. *Highlights tumor cell clones in which *Agt* is significantly over-expressed.

(C) Relative mRNA expression levels of colony-stimulating factor (*Csf*)*-1*, *Csf-2*, angiotensinogen (*Agt*), interferon gamma (*Ifng)*, interleukin 1-beta (*Il1b)* and tumor necrosis factor- alpha (*Tnfa*) were measured by quantitative real time PCR in tumor-involved (n=3-5) and uninvolved (n=3-5) lung tissue isolated from KP tumor-bearing mice at 12 wk post tumor initiation. Lung tissues of tumor-free mice (n=3-5) served as controls.

(D) Relative AngII levels (measured by ELISA) detected in the supernatant of lung tissue primary cultures. The primary cultures consisted either of excised KP tumor nodules (n=6; each bar represents a distinct tissue biopsy) or excess control tissue (n=2). Cell suspensions were prepared from each nodule and control tissue and similar number of cells were plated and kept in RPMI 1640 medium supplemented with 10% FBS for 3 d in a humidified incubator at 37 C and 5 % CO2. The number of living cells after 3 days of culture was comparable in all cultures. Data are normalized to AngII levels found in the supernatant of control tissues.

(E) Top: Relative *AGT* mRNA expression levels (quantitative real time PCR) in 2 human and 2 mouse tumor cell lines. Data are normalized to *AGT* mRNA expression levels in tumor-free mouse lung tissue. Bottom: AGT protein secretion (ELISA) and by the same cell lines cultured in conditioned medium.

(F) Left: Representative examples of AGT (top), CD68 (middle) and CD163 (bottom) expression in lung biopsies in which AGT expression is increased in tumor involved tissue (2 of 13 patients are shown; patients 8H6 and 8H2). Right: AGT (top), CD68

(middle) and CD163 (bottom) expression in control uninvolved tissue obtained from two different donors (patients 8E6 and 8A1). Scale bar represents 50 μm.

(G) Microarray data mining of NSCLC clinical specimens using the Oncomine platform. The heatmap shows *AGT* mRNA over-expression or under-expression in NSCLC tissue vs. normal tissue in 11 datasets (more information about each dataset is available in panel H). Each color-coded box shows the median rank (%) of *AGT* mRNA expression within the transcriptome for each dataset (for example, "10%" indicates that the gene is ranked in the top (red) or bottom (blue) 10% of the transcriptome). The p-Values are based on comparisons of *AGT* mRNA ranking in NSCLC tissue vs. normal tissue across all 11 datasets (see also panel H).

(H) Microarray datasets used to analyze *AGT* mRNA expression in panel G. "Index": Datasets numbered from 1 to 11 as in Fig. 7F; "NSCLC subtype": NSCLC subtype for each data set; "Fold change": fold change expression for *AGT* mRNA for each data set; "p-Value": p-value refers to expression analysis for each data set; "Gene rank": values refer to expression analysis; "Reference": citations for each microarray dataset.

(I) The Kaplan-Meier curve compares overall survival of NSCLC patients according to *AGT* mRNA expression in tumor tissue at time of diagnosis. Patients were operationally divided according to *AGT* expression and the survival curve was generated by comparing survival between the 20% patients with highest *AGT* levels (AGT^{hi}; n= 46) and the 20% patients with lowest *AGT* levels (AGT^{lo}; n= 46). Patients' data were obtained from Nguyen et al., Cell, 2009;138:51-62. Demographic and clinical characteristic of the patients are shown in Table S1.

(J) Microarray data mining of NSCLC clinical specimens using the Oncomine platform. The heatmap shows *AGT* gene copy number gain or loss in NSCLC tissue vs. normal tissue in 5 datasets (additional information is available in supplemental materials and methods). Each color-coded box shows the median rank (%) of *AGT* copy number gain or loss expression within the genome for each dataset. The p-Values are based on comparisons of *AGT* gene ranking in NSCLC tissue vs. normal tissue across all 5 datasets.

Data in panels A-E are presented as mean ± SEM. *, $p<0.05$.

Table S1 – Demographic and clinical characteristics of two cohorts of patients with lung adenocarcinoma[a]

Variable	AGT^{hi} (n=46)	AGT^{lo} (n=46)	P Value
Median age (range) — yr	65 (43-86)	67.5 (37-83	0.8473
Male sex — %	50	50	0.6679
Smoking history — %			0.6062
Currently smoking	9	7	
Never smoked	26	25	
Smoked in the past	14	18	
Unknown	1	0	
Pathologic N stage — %			0.0239
N0	27	40	
N1	13	4	
N2	10	5	
Pathologic T stage — %			0.3085
T1	25	22	
T2	20	26	
T3	2	0	
T4	3	2	
Histologic grade — %			0.6501
Moderate differentiation	8	9	
Poorly differentiated	12	8	
Well differentiated	2	4	
Unknown	28	29	
Stage — %			0.1044
1A	9	12	
1B	3	11	
2A	3	0	
2B	2	0	
3A	5	2	
3B	3	1	
4	1	2	
Unknown	23	22	
Adjuvant chemotherapy — %			0.4353
No	14	17	
Yes	9	4	
Unknown	27	28	
Adjuvant radiation therapy — %			0.9220
No	18	18	
Yes	4	3	
Unknown	27	28	

[a]Contingency table comparing clinical covariates corresponding to the pooled top 20% highest *AGT* expressors (AGT^{hi}) and bottom 20% lowest *AGT* expressors (AGT^{lo}) that were obtained from the analysis of two independent microarray data sets (MSKCC set 1 and set 2; Nguyen et al. 2009) and were used for survival analysis presented in **Fig 6F**. Median age is shown in years (yr) and all other variables are presented as the fraction (%) from the total number of patients for each cohort (AGT^{hi} or AGT^{lo}). P value refers to the comparison of each variable using either the Fisher's exact test, chi-squared or the unpaired 2-tailed Student's t test. See Supplemental Experimental Procedures below for more information about data analysis.

SUPPLEMENTAL EXPERIMENTAL PROCEDURES

mAbs for flow cytometry

The following antibodies were used: PE-conjugated anti-CD90 (clone 53-2.1; BD Biosciences), PE-conjugated anti-B220 (clone RA3-6B2; BD Biosciences), PE-conjugated anti-CD49b (clone DX5; BD Biosciences), PE-conjugated anti-NK1.1 (clone PK136; BD Biosciences), PE-conjugated anti-Ly-6G (clone 1A8; BD Biosciences), PE-conjugated anti-CD19 (clone 1D3; BD Pharmingen), PE-conjugated anti-CD11b (clone M1/70; BD Pharmingen), PE-conjugated anti-CD11c (clone N418; eBioscience), APC-conjugated anti-CD11b (clone M1/70; BD Biosciences), APC-Cy7-conjugated anti-CD11b (clone M1/70; BD Biosciences), PE-Cy7-conjugated anti-F4/80 (clone BM8; BD Biosciences), Alexa Fluor 700-conjugated anti-CD11c (clone HL3; BD Biosciences), APC-conjugated anti-CD117 (clone 2B8; BD Biosciences) APC-Cy7-conjugated anti-CD16/32 (clone 2.4G2; BD Biosciences), PE-Cy7-conjugated anti-Sca1 (clone D7; eBiosciences), Alexa Fluor 700-conjugated anti-CD34 (clone RAM34; BD Biosciences), FITC-conjugated anti-CD34 (clone RAM34; BD Biosciences), PE-conjugated anti-CD127(IL-7Ra) (clone A7R34; eBiosciences), FITC-conjugated anti-BrdU (BD Biosciences), APC-conjugated anti-BrdU (BD Biosciences), APC-conjugated anti-CD45.1 (clone A20; BD Biosciences), PerCP-Cy5.5-conjugated anti-CD45.2 (clone 104; BD Biosciences), biotin-conjugated anti-mouse VEGF (clone AAM51B; Serotec), APC-conjugated anti-mouse TNF (BD Pharmingen), FITC-conjugated anti-mouse CD62L (clone MEL-14; BD Pharmingen), biotin-conjugated anti-CD115 (clone AFS98; BD Biosciences), PerCP-conjugated streptavidin (BD Biosciences).

For progenitor staining the lineage ('Lin') antibody mix included the following PE-conjugated antibodies: anti-CD90, anti-B220, anti-CD19, anti-CD49b, anti-NK1.1, anti-Ly-6G, anti-CD11b, anti-CD11c, and anti-CD127. For cell labeling, single cell suspensions were typically incubated for 30 min at 4°C with appropriate antibodies in PBS supplemented with 1% fetal bovine serum (FBS). For cell cycle analysis, the FXCycle Violet stain reagent was used following the manufacturer's protocol (Invitrogen).

Histology

For detection of Angiotensinogen (Agt) in mouse lung tissue, serial paraffin-embedded sections were prepared and all sections were incubated in 1% hydrogen peroxide solution to block endogenous peroxidase activity before antibody staining. Sections were then labeled with an anti-mouse/rat Agt rabbit antibody (clone 405; Immuno-Biological Laboratories, IBL) and then with a biotinylated anti-rabbit IgG antibody (Vector Laboratories) to detect the primary antibody. Vectastain ABC kit (Vector Laboratories, Inc.) and a 3-amino-9-ethylcarbazole (AEC) substrate (Dako) were used for color development and all sections were counterstained with Harris hematoxylin solution (Sigma Aldrich).

For detection of Agt in human lung tissue, paraffin embedded lung sections were obtained at Massachusetts General Hospital from 44 patients with stage 1 lung adenocarcinoma. Paraffin-embedded tissue sections were deparaffinized and rehydrated prior to the antigen retrieval procedure. Proteinase K (Dako) was used for the proteolytic digestion, and then heat-induced epitope retrieval was performed using retrieval solution (pH6.0) (BD Biosciences), according to the manufacturer's protocol. The sections were incubated in 1% hydrogen peroxide solution to block endogenous peroxidase activity and stained with goat anti-human Serpin A8/Angiotensinogen antibody (R&D systems). Normal goat IgG antibody was used as an isotype control (R&D Systems). Biotinylated anti-goat IgG (H+L) was used as secondary antibody. Vectastain ABC kit (Vector Laboratories, Inc.) and a 3-amino-9-ethylcarbazole (AEC) substrate (Dako) were used for color development and all sections were counterstained with Harris hematoxylin solution (Sigma Aldrich). Human liver tissue was used as positive control for Agt staining.

For detection of macrophages in human lung tissue, paraffin-embedded sections were deparaffinized and rehydrated before the antigen retrieval procedure. Antigen retrieval was done as described above. Lung tissue sections were stained with mouse anti-human CD68 (clone: KP1, Dako) and mouse anti-human CD163 (clone: EDHu-1, AbD serotec) mAbs. Biotinylated anti-mouse IgG (H+L) (Vector Laboratories, Inc.) was used as secondary antibody. Vectastain ABC kit (Vector Laboratories, Inc.) and a 3-amino-9-ethylcarbazole (AEC) substrate (Dako) were used for color development and all sections were counterstained with Harris hematoxylin solution (Sigma Aldrich).

Slide images were captured and digitized automatically at a magnification of 40x (NanoZoomer 2.0RS, Hamamatsu, Japan).

Continuous delivery of AngII and hydralazine into mice

Osmotic minipumps (Alzet, Durect Corp.) were loaded either with AngII (Bachem) dissolved in PBS containing 0.14% acetic acid (Swirski et al., 2009) or with hydralazine dissolved in water. Minipumps were preincubated for 48 h in PBS at 37°C to assure immediate delivery of AngII or hydralazine after implantation. Female C57BL/6 mice were implanted subcutaneously at the dorsum of the neck with the loaded osmotic minipumps. AngII and hydralazine were delivered at a rate of 0.25 µl/hour at 1.5 mg/kg/day and 15 mg/kg/day, respectively. Tumor-free mice received AngII at a dose that replicated the plasma concentration found in tumor-bearing mice.

Measurement of AngII levels in peripheral blood

Blood was collected from control and KP mice at week 11-12 post tumor initiation. Blood was drawn from mice under anesthesia by cardiac puncture with a syringe pre-loaded with 80 μl of 100 mM EDTA anticoagulant. The blood was transferred to an eppendorf tube containing 50 μl of protease inhibitor cocktail VI (Research Product Inc.), supplemented with 50 mM p-hydroxymercuribenzoid acid (Sigma), centrifuged, and the supernatant was loaded onto Amprep Phenyl PH mini-columns (GE Biosciences) to isolate peptides from the sera. Methanol-eluted peptides were dried by vacuum centrifugation. AngII concentration was determined with an AngII ELISA (Cayman Chemical), and normalized to the volume of blood or cell culture supernatant collected.

Blood pressure measurements

Blood pressure was monitored with a noninvasive tail cuff CODA System (Kent Scientific) as described previously (Daugherty et al., 2009).

Bone marrow chimeras

Wild-type C57BL/6 mice were reconstituted with syngeneic bone marrow cells from either wild-type or *Agtr1a*$^{-/-}$ mice. *Agtr1a*$^{-/-}$ mice were also reconstituted with syngeneic bone marrow cells from wild-type mice. On the day of bone marrow transplantation, recipient animals were lethally irradiated with a ^{137}Cs source (Gammacell 40 Excactor, MDS Nordion) using a dose of 9.8 Gy. Animals were injected with the respective donor cells within 4-6 h post irradiation. Each animal received 5x10^4 enriched hematopoietic progenitor cells (defined as [Gr-1, NK1.1/B220/CD11b/CD11c/ Ly-6C/Ly-6G/Ter119]$^-$ c-Kit$^+$ and Sca-1$^+$), which were sorted (FACS Aria) from pooled spine, hipbones, femur and tibia of donor animals. Recipient animals were monitored for proper reconstitution of the hematopoietic system 10-12 weeks later.

Parabiosis

Parabiosis experiments used weight- and sex-matched C57BL/6 and C57BL/6 *EGFP* mice (AngII-treated mice) and 129 and 129 *EYFP* mice (KP tumor-bearing mice). Mice were anesthetized with isoflurane and then joined by a technique adapted from Bunster and Meyer (Bunster and Meyer, 1933). Briefly, after shaving the corresponding lateral side of each mouse, matching skin incisions were made from behind the ear to the tail of each mouse and the subcutaneous fascia were bluntly dissected to create about 0.5 cm of free skin. The olecranon and knee joints were attached by a mono-nylon 5.0 suture (Ethicon) and the dorsal and ventral skins were approximated by continuous suture. Mice were surgically separated after 14-30 d by a reversal of the procedure.

Percentage chimerism for each studied cell population was calculated as %EGFP$^+$ / (%EGFP$^+$ + %EGFP$^-$) in C57BL/6 mice, and as %EGFP$^-$ / (%EGFP$^+$ + %EGFP$^-$) in GFP mice. Likewise, percentage chimerism for each studied cell population was calculated as %EYFP$^+$ / (%EYFP$^+$ + %EYFP$^-$) in 129 mice, and as %EYFP$^-$ / (%EYFP^{++} + %EYFP$^-$) in EYFP mice.

Mouse progenitor cell culture and cell proliferation assay

Mouse progenitor cells obtained by fluorescence-activated cell sorting (FACS Aria) were cultured in Serum-Free Expansion Medium (SFEM, StemCell Technologies) supplemented with 10% FBS (Valley Biomedical) in a humidified incubator at 37°C, 5% CO_2. Proliferation of GMPs was assessed in the presence or absence of either AngII (10 μM, Bachem) or GM-CSF (1 ng/mL, Peprotech) over the course of 48 h and using the enzyme-based ViaLight Kit (Lonza) as described previously (Rieger et al., 2009). Readings were performed on a Safire2 microplate reader (Tecan). Relative luminescence units were normalized to the number of cells initially plated.

Colony forming cell assay

To determine the presence and number of macrophage colony-forming units (CFU-M), murine cells were cultured in appropriate complete methylcellulose-based medium (MethoCult GF M3434 from StemCell Technologies) in 6-well plates. Colony numbers and morphology were assessed after 10-14 d of culture.

S1P chemotaxis assay

Murine Lin$^-$ CD117$^+$ cells were isolated (FACS Aria) from the bone marrow of C57BL/6 mice that were previously infused with AngII for 8 d. The cells were seeded at a density of 1x10^5 cells/well on uncoated, tissue culture treated, 3 µm pore size transwell plates (BD Biosciences). Cell transmigration into the bottom chamber was assessed in response to 100 nM S1P (Sigma-Aldrich), CXCL12/SDF-1α (50 nM, Peprotech) or in medium alone (RPMI + 10% FCS) as described previously (Massberg et al., 2007). The plates were incubated for 3 h at 37°C, 5% CO_2 in a tissue culture incubator. Before further processing, 2x10^5 microspheres were added to the bottom wells as an internal counting standard (PolySciences, Inc.). For each sample 1x10^5 events were acquired on a LSRII flow cytometer (BD Biosciences) and absolute counts of transmigrated cells were calculated based on the added calibration beads according to the manufacturer's protocol. The chemotactic index was calculated as the number of cells that migrated towards the S1P gradient, divided by the number of cells that migrated in the absence of the chemoattractant (Massberg et al., 2007).

Losartan, enalapril and FTY720 treatments

Tumor-bearing KP mice were injected i.p. with daily doses of 20 mg/kg Losartan potassium (USP Rockville) for 7 d. Tumor-bearing mice received enalapril maleate (Sigma-Aldrich) through daily i.p. injections or by food intake for survival studies (5 or 50 mg/kg, Harlan). C57BL/6 mice were injected i.p. with daily doses of 3 mg/kg FTY720 (Cayman Chemical) for 7 d.

Design and use of retroviral vectors for constitutive $S1P_1$ expression in HSCs

The untagged full-length cDNA clone of *S1p1 (S1pr1, Edg1)* (Gene Bank BC049094.1) was obtained from OriGene and cloned into the multiple cloning site upstream of an IRES in a MSCV2.2-IRES-EGFP retroviral vector using oligos introducing a 5' BglII site before the start codon and a 3' EcoRI site after the stop codon, respectively. Retroviral particles were produced in 293T cells co-transfected with either an empty control or the *S1p1* expressing retroviral vector and the EcoPak packaging vector (Gavrilescu and

Van Etten, 2007) using the TransIT-LT1 transfection agent (Mirus). The transfection medium was replaced after 24 h and viral supernatants were collected 24 h thereafter, filtered through a 0.22 µm syringe filter and used directly for transfection of HSCs.

0.5-1x10^5 HSCs were purified (FACS Aria) and plated into a retronectin-coated (Takara) well of a 6 well plate and transduced over night with 200 µl retroviral supernatant in 1ml stem cell media supplemented with 4 µg/ml polybrene (American Bioanalytical Inc.). The media composition consisted of RPMI (Mediatech Inc.) supplemented with 10% FCS (stem cell grade, Stem Cell Technologies), 1 µg/ml mSCF (Peprotech), 0.5 µg/ml TPO (Peprotech), 0.5 µg/ml Flt3-L (Peprotech), 0.2 µg/ml IL-3 (Peprotech), 100 U/ml Pen/Strep (Mediatech Inc.) and 2 mM L-Glutamine (Mediatech Inc.). The cells were subsequently expanded over 3 d in fresh stem cell medium. Transduction efficiency (usually >80%) was assessed by flow cytometry prior to injection based on EGFP expression and specific expression or silencing of the gene of interest was assessed by Taqman real-time PCR using gene specific primers and by flow cytometry using an anti-S1P1 antibody.

Spleen transplantation

Spleen transplants were performed using donor *EYFP* 129 mice and recipient 129 mice at 7 weeks post injection with KP tumor cells. The surgical procedure of spleen transplantation and the enumeration of cells that deployed from the donor spleen to distant tissue were performed as previously described (Swirski et al., 2009). Briefly the side branches of spleen/pancreas vessels were carefully ligated and supra renal aorta and portal vein cuffs of the donor were prepared for micro-anastomosis. The spleen of the recipient mouse was removed after ligature of the vessels with silk 6-0. The recipient infrarenal aorta and inferior vena cava were clamped, opened longitudinally and end-to-side anastomoses were established with the donor aortic and portal cuffs using 10-0 Ethillon suture. The time of ischemia of the donor spleen, which ended after completion of both vascular anastomoses by unclamping the recipient aorta and vein, was ~60 min. After unclamping, blood flow through the transplanted organ was verified visually, followed by splenectomy of the orthotopic recipient spleen. The procedure was performed under isoflurane anesthesia.

Quantitative real-time PCR

The following primers and probes were used according to the manufacturer's instructions: *AGT* (Hs00174854_m1), *Agt* (Mm00599662_m1), *S1p1* (*S1pr1, Edg1*) (Mm02619656_s1), *Csf1* (Mm00432688_m1), *Csf2* (Mm01290062_m1), *Ifng* (Mm00801778_m1), *Il-1b* (Mm00434228_m1), *TNF* (Mm00443258_m1) (all from Applied Biosystems). Reactions were run on an ABI 7100 or ABI 7500 Fast Real-Time PCR machine (Applied Biosystems) in triplicate 20 µl reactions using standard machine settings. Expression data were normalized using 18s rRNA endogenous control (Hs99999901_s1) and relative expression values were calculated using the qGene module for Excel (Muller et al., 2002).

Analysis of human microarray data

To compare *AGT* mRNA expression between tumor-involved and non-involved tissue, we filtered Oncomine datasets for the following parameters: Gene: *AGT*; Analysis Type: Cancer vs. Normal Analysis; Cancer Type: Non-Small Cell Lung Carcinoma; Data Type: mRNA; Sample Type: Clinical Specimen. We then selected and compared all the resulting 11 datasets (See also **Fig. S6H**).

To assess *AGT* gene copy number in cancer patients, we filtered Oncomine datasets for the following parameters: Gene: *AGT*; Analysis Type: Differential Analysis; Cancer Type: Lung Cancer; Data Type: DNA; Sample Type: Clinical Specimen. We then selected and compared all the resulting 5 datasets published in Beroukhim et al., 2010, Jaiswal et al., 2009 and from a public entry available on the Oncomine database (TCGA, no associated paper, 2011).

To assess survival in NSCLC patients with either high or low *AGT* levels, we obtained two datasets from previously published work by Nguyen et al. 2009 (**Fig. 6F**; 'MSKCC set 1 and set 2'). Raw expression data (CEL files) for each dataset were obtained and normalized independently with the Gene Pattern ExpressionFileCreator module using the RMA method with quantile normalization and background correction (Reich et al., 2006). Thereafter we ranked the patients according to *AGT* expression in each dataset and selected the top 20% highest *AGT* expressors (n=46) and bottom 20% lowest *AGT* expressors (n=46). Kaplan-Meier survival curve was generated by pooling the selected data.

SUPPLEMENTAL REFERENCES

Beer, D.G., Kardia, S.L., Huang, C.C., Giordano, T.J., Levin, A.M., Misek, D.E., Lin, L., Chen, G., Gharib, T.G., Thomas, D.G. et al. (2002). Gene-expression profiles predict survival of patients with lung adenocarcinoma. Nat Med *8*, 816–824.

Beroukhim, R., Mermel, C.H., Porter, D., Wei, G., Raychaudhuri, S., Donovan, J., Barretina, J., Boehm, J.S., Dobson, J., Urashima, M. et al. (2010). The landscape of somatic copy-number alteration across human cancers. Nature *463*, 899–905.

Bhattacharjee, A., Richards, W.G., Staunton, J., Li, C., Monti, S., Vasa, P., Ladd, C., Beheshti, J., Bueno, R., Gillette, M. et al. (2001). Classification of human lung carcinomas by mRNA expression profiling reveals distinct adenocarcinoma subclasses. Proc Natl Acad Sci U S A *98*, 13790–13795.

Bunster, E., and Meyer, R.K. (1933). An improved method of parabiosis. *The Anatomical Record 57*, 339–343.

Daugherty, A., Rateri, D., Hong, L., and Balakrishnan, A. (2009). Measuring blood pressure in mice using volume pressure recording, a tail-cuff method. J Vis Exp

Garber, M.E., Troyanskaya, O.G., Schluens, K., Petersen, S., Thaesler, Z., Pacyna-Gengelbach, M., van de Rijn, M., Rosen, G.D., Perou, C.M., Whyte, R.I. et al. (2001). Diversity of gene expression in adenocarcinoma of the lung. Proc Natl Acad Sci U S A *98*, 13784–13789.

Gavrilescu, L.C., and Van Etten, R.A. (2007). Production of replication-defective retrovirus by transient transfection of 293T cells. J Vis Exp 550.

Hou, J., Aerts, J., den Hamer, B., van Ijcken, W., den Bakker, M., Riegman, P., van der Leest, C., van der Spek, P., Foekens, J.A., Hoogsteden, H.C. et al. (2010). Gene expression-based classification of non-small cell lung carcinomas and survival prediction. PLoS One *5*, e10312.

Jaiswal, B.S., Janakiraman, V., Kljavin, N.M., Chaudhuri, S., Stern, H.M., Wang, W., Kan, Z., Dbouk, H.A., Peters, B.A., Waring, P. et al. (2009). Somatic mutations in p85alpha promote tumorigenesis through class IA PI3K activation. Cancer Cell *16*, 463–474.

Landi, M.T., Dracheva, T., Rotunno, M., Figueroa, J.D., Liu, H., Dasgupta, A., Mann, F.E., Fukuoka, J., Hames, M., Bergen, A.W. et al. (2008). Gene expression signature of cigarette smoking and its role in lung adenocarcinoma development and survival. PLoS One *3*, e1651.

Massberg, S., Schaerli, P., Knezevic-Maramica, I., Köllnberger, M., Tubo, N., Moseman, E.A., Huff, I.V., Junt, T., Wagers, A.J., Mazo, I.B. et al. (2007). Immunosurveillance by hematopoietic progenitor cells trafficking through blood, lymph, and peripheral tissues. Cell *131*, 994–1008.

Muller, P.Y., Janovjak, H., Miserez, A.R., and Dobbie, Z. (2002). Processing of gene expression data generated by quantitative real-time RT-PCR. Biotechniques *32*, 1372–4, 1376, 1378-9.

Nguyen, D.X., Chiang, A.C., Zhang, X.H., Kim, J.Y., Kris, M.G., Ladanyi, M., Gerald, W.L., and Massague, J. (2009). WNT/TCF signaling through LEF1 and HOXB9 mediates lung adenocarcinoma metastasis. Cell *138*, 51–62.

Rieger, M.A., Hoppe, P.S., Smejkal, B.M., Eitelhuber, A.C., and Schroeder, T. (2009). Hematopoietic cytokines can instruct lineage choice. Science *325*, 217–218.

Stearman, R.S., Dwyer-Nield, L., Zerbe, L., Blaine, S.A., Chan, Z., Bunn, P.A.J., Johnson, G.L., Hirsch, F.R., Merrick, D.T., Franklin, W.A. et al. (2005). Analysis of orthologous gene expression between human pulmonary adenocarcinoma and a carcinogen-induced murine model. Am J Pathol *167*, 1763–1775.

Su, L.J., Chang, C.W., Wu, Y.C., Chen, K.C., Lin, C.J., Liang, S.C., Lin, C.H., Whang-Peng, J., Hsu, S.L., Chen, C.H. et al. (2007). Selection of DDX5 as a novel internal control for Q-RT-PCR from microarray data using a block bootstrap re-sampling scheme. BMC Genomics *8*, 140.

Swirski, F., Nahrendorf, M., Etzrodt, M., Wildgruber, M., Cortez-Retamozo, V., Panizzi, P., Figueiredo, J.L., Kohler, R.H., Chudnovskiy, A., Waterman, P. et al. (2009). Identification of splenic reservoir monocytes and their deployment to inflammatory sites. Science *325*, 612–616.

Yamagata, N., Shyr, Y., Yanagisawa, K., Edgerton, M., Dang, T.P., Gonzalez, A., Nadaf, S., Larsen, P., Roberts, J.R., Nesbitt, J.C. et al. (2003). A training-testing approach to the molecular classification of resected non-small cell lung cancer. Clin Cancer Res *9*, 4695–4704.